Acta Physiol Scand 2000, **168**, 615–622

Near-infrared spectroscopy for monitoring muscle oxygenation

R. BOUSHEL[1] and C.A. PIANTADOSI[2]

1 Sports Medicine Research Unit, Department of Rheumatology, Bispebjerg Hospital, Copenhagen Denmark
2 Division of Pulmonary and Critical Care Medicine, Department of Medicine, Duke University Medical Center, Durham, North Carolina, USA

ABSTRACT

Near-infrared spectroscopy (NIRS) is a non-invasive method for monitoring oxygen availability and utilization by the tissues. In intact skeletal muscle, NIRS allows semi-quantitative measurements of haemoglobin plus myoglobin oxygenation (tissue O_2 stores) and the haemoglobin volume. Specialized algorithms allow assessment of the oxidation–reduction (redox) state of the copper moiety (CuA) of mitochondrial cytochrome c oxidase and, with the use of specific tracers, accurate assessment of regional blood flow. NIRS has demonstrated utility for monitoring changes in muscle oxygenation and blood flow during submaximal and maximal exercise and under pathophysiological conditions including cardiovascular disease and sepsis. During work, the extent to which skeletal muscles deoxygenate varies according to the type of muscle, type of exercise and blood flow response. In some instances, a strong concordance is demonstrated between the fall in O_2 stores with incremental work and a decrease in CuA oxidation state. Under some pathological conditions, however, the changes in O_2 stores and redox state may diverge substantially.

Keywords blood flow, muscle oxygenation, near infrared.

Received 28 November 1999, accepted 9 December 1999

Although optical methods have been used for many years for investigating muscle metabolism *in situ*, most techniques in use before 1977 required surgical exposure of the tissue. At that time, Frans Jobsis (1977) demonstrated the feasibility of using near-infrared spectroscopy (NIRS) to assess the adequacy of oxygen provision and utilization in living tissues. The NIRS technique is non-destructive, continuous and operates in real time, thus lending itself to *in vivo* monitoring of tissue oxygenation. Near-infrared spectroscopy has been used primarily as a research tool to assess dynamic changes in the status of tissue oxyhaemoglobin ($tHbO_2$), deoxy-haemoglobin (tHb), total blood (haemoglobin) volume (tBV) and the oxidation state of the copper moiety (CuA) of mitochondrial cytochrome c oxidase (cytochrome a,a_3) in brain and muscle. Recently, using tracers that absorb near-infrared light, it has also become possible to quantitate blood flow through an illuminated region of living tissue. Near-infrared spectroscopy instrumentation has been improved over the years in terms of design and computational software for real time analysis of NIR absorption spectra and the optical principles, pitfalls and limitations are readily appreciated by physiologists.

Near-infrared spectroscopy is based on the relative ease with which near-infrared light (700–1000 nm) passes through biological tissues, including bone, skin and muscle. The amount of light recovered after illuminating the tissue depends on the degree of scattering in the tissue and the amount of absorption by the chromophores in the tissue. Only three molecules are known to affect NIR light absorption during changes in tissue oxygen tension, haemoglobin, myoglobin and cytochrome c oxidase. Differences in the oxygen-dependent absorption spectra of the iron and/or copper centres of these molecules make it possible to measure changes in the relative amounts of oxidized copper and oxygenated haeme species present in muscle (Jobsis 1977). In most cases, however, NIRS does not allow for precise quantitative measurement of concentration differences but instead provides trends in the responses of the oxylabile chromophores to changes in oxygen availability.

The approximate tissue concentrations of oxy- and deoxy-haemoglobin have been estimated by measuring the optical pathlength of NIR photons traversing the tissues (Wyatt *et al.* 1990, van der Zee *et al.* 1992). The

Correspondence: Robert Boushel DSc, Bispebjerg Hospital, Bispebjerg Bakke 23, 2400 Copenhagen NV, Denmark.

principles involved can be demonstrated by examining the relationship between absorption and chromophore concentration in the Beer–Lambert Law modified for scattering media: $A = \varepsilon[c]LB + G$, where A is the absorption of light expressed as optical density, ε the extinction coefficient of the chromophore, [c] the chromophore concentration, L the distance between the point of light entry and exit (optode separation), B the pathlength resulting from scatter in the tissue and G is a lumped parameter related to tissue and optode geometry. The extinction coefficients can be estimated easily by direct measurement and estimates of B can be obtained using time-resolved or time-of-flight analysis (TOFA) optical measurements. Values for B are only approximate and vary to some extent with changes in absorption by the tissue chromophores. Values of G are difficult to determine, hence absolute concentration values have been difficult to determine accurately. Despite the problems of measuring pathlength and geometry, their contributions to light attenuation in tissues can generally be assumed to be constant for a fixed optode position thereby allowing both trend information and relative concentration differences to be acquired. In skeletal muscle, a full range of oxygenation conditions can be exploited to provide both maximum and minimum spectral values (total labile signal or TLS) during hyperaemia and ischaemia to allow reproducible calibration of the measurements (Piantadosi 1993).

Several types of NIRS equipment exist and are now available commercially. Widespread acceptance of NIRS, however, has been slow because equipment, geometry and software algorithms have not yet been standardized. Important differences include wavelength selection, number of wavelengths, optode spacing and geometry, the nature of the algorithms used to deconvolute overlapping absorption spectra and the rigour applied to validating the algorithms. These points are critically important, for example, when determining the contribution of CuA to an overall change in tissue NIR signals. The maximum contribution of CuA compared with that of HbO_2 only amounts to 10–15% of the total labile signal in muscle tissue.

Most biophysical investigations of NIRS indicate that a minimum of four wavelengths are necessary to generate algorithms for NIRS. Coefficients are used at each wavelength to deconvolute the overlapping absorption spectra of oxyhaemoglobin, deoxyhaemoglobin and CuA. The coefficients are derived by matrix operations on sets of absorption values from either *in vivo* spectra obtained independently using the same geometry (Piantadosi 1993) or from *in vitro* spectra using light-scattering tissue models (Wray *et al.* 1988). The algorithms are also of two types: those used only for trend monitoring (equations set up for equal signals for each species) and those scaled to assess relative concentrations (Piantadosi *et al.* 1997). The wavelengths and coefficients used in the laboratory at Duke for the latter purpose are shown in Table 1. Finally, NIRS signals from skeletal muscle include contributions from oxy- and deoxy-myoglobin in addition to those of oxy- and deoxy-haemoglobin because the NIR spectra of the oxy- and deoxy- forms of the two molecules are indistinguishable. In even red skeletal muscle, however, the majority of the NIRS O_2 store signal is still derived from oxy- and deoxy-haemoglobin.

Table 1 Specific extinction coefficients for NIRS applications in muscle

Application	λ	$tHbO_2$ + MbO_2	thb	CuA	ICG
Spectroscopy	775	−1.519	2.208	−0.658	–
	810	0.576	−0.919	1.384	–
	870	−0.236	0.186	−0.140	–
	904	1.483	−0.864	−0.513	–
Blood flow	775	0.7034	1.2474	–	0.130
	813	0.9142	0.7641	–	0.151
	850	1.0549	0.7151	–	0.017
	913	1.0579	0.6987	–	0.003

Optode positioning is important to assure appropriate penetration of photons to deep muscle, avoid stray and short path light and prevent recording primarily from more superficial structures. These goals are most easily accomplished using a reflectance mode wherein the source and detector fibre optic bundles are spaced several centimetres apart on the skin overlying the belly of the muscle. When evaluating changes in the oxygenation of muscle, it is important to consider the contribution of the skin to the NIRS signal. The contribution of skin overlying muscle has been shown to be less than 5% of the total signal strength in the cat (Piantadosi *et al.* 1986). The same is true of the human forearm when light pressure is applied to the skin with the optodes (Hampson & Piantadosi 1988).

Recent advances in technology

Significant progress has been made over the past decade in determining how far NIR light travels in living tissue. Time-of-flight analysis (TOFA) using picosecond pulses of light, phase-modulated spectroscopy and Monte Carlo simulations have been used to estimate pathlength, path geometry and the relative contributions of tissues superficial to the area of interest (Hirako *et al.* 1993). For instance, TOFA has indicated the pathlength through brain tissue is four to six times the separation distance between the source and the receiving optodes (2,3). We find values of close to four in red muscle (C.A. Piantadosi, unpublished

observations). The ability to estimate pathlength in real time is highly desirable but still somewhat impractical and frequently an average pathlength factor is applied to the data from an entire study. Using phase-modulated spectroscopy, Kurth *et al.* (1993) have pointed out that constant scatter and pathlength in a given subject may be a reasonable assumption but there is a significant intersubject variability, making concentration measurements obtained in this way potentially inaccurate. Benaron & Stevenson (1994) have reported that a twofold difference in pathlength between different wavelengths of NIR light could be carried through computations into a twofold over- or underestimate of haemoglobin concentration.

Measurement of regional blood flow by NIRS

The ability to measure local blood flow through a portion of tissue illuminated by NIR light adds substantially to the information obtained on the adequacy of cellular oxygen provision. Blood flow is required to determine regional oxygen delivery and oxygen uptake. Use of a detectable 'tracer' and the Fick principle makes flow estimates possible. The rate of accumulation of a tracer in the tissue to be studied is equal to its rate of inflow minus its rate of outflow. If a tracer is introduced rapidly and its rate of accumulation measured with respect to time, blood flow can be measured as a ratio of the tracer accumulated to the quantity of tracer introduced over a given time. The first NIR application of this technique was reported in 1981 by Colacino *et al.* (1981) in the brain of the duck using indocyanine green (ICG) dye as a tracer. Indocyanine green is a water-soluble tricarbocyanine dye that is strongly protein bound (95%) in blood and absorbs NIR light at an absorption maximum near 800 nm. Indocyanine green has a relatively short half-life (≈5 min) making it nearly ideal for blood flow measurements using NIRS.

Colacino *et al.* (1981) found a good correlation in cerebral blood flow (CBF) measurements made by xenon clearance and those by NIRS using ICG. They pointed out practical advantages of the NIR technique such as low cost, lack of toxicity, no need for radioactive materials and ease of repeatability. Additionally, flow information could be obtained almost simultaneously with other indicators of tissue oxygenation including haemoglobin oxygenation and CuA redox state. Other groups have also reported the utility of NIRS in combination with ICG to quantify cerebral blood flow (Roberts *et al.* 1993, Kuebler *et al.* 1998).

Indocyanine green dye clearance curves were first recorded by NIRS from intact skeletal muscle as early as 1986 (Piantadosi *et al.* 1986). Quantification of muscle blood flow using ICG during exercise in humans has recently been reported (Boushel *et al.* 1997, 1999). Relative to conventional methods for limb blood flow measurements during exercise, NIRS may be advantageous for detecting patterns of blood flow in discrete regions within a limb owing to its potential to provide spatial resolution.

Attempts to eliminate the need for an exogenous tracer have led others to monitor abrupt change in HbO_2 as a tracer detectable by NIRS (Edwards *et al.* 1988, 1993, Skov *et al.* 1991, Bucher *et al.* 1992). Although the convenience of this approach is attractive, it comes with stringent requirements. First, a significant step change in tissue HbO_2 must be introduced and detected. Second, detection of abrupt changes in HbO_2 requires simultaneous determination of arterial haemoglobin saturation, e.g. by pulse oximetry. As HbO_2 (by NIRS) and pulse oximetry are performed at two different sites, the time delay between blood flow to the two sites must be accounted for in calculations. These measurements also assume a constant pathlength of light (used to determine HbO_2 concentration) and require modification by a constant, to account for the concentration of haemoglobin in the circulation. Large vessel haematocrit is generally greater and may vary in its relationship to microvascular haematocrit; the latter is more relevant to signals acquired by NIRS. Notwithstanding these potential problems, two studies have correlated NIRS blood flow measurements with xenon techniques with a reasonable degree of accuracy (Skov *et al.* 1991, Bucher *et al.* 1992).

Human forearm muscle blood flow by NIRS has been compared with venous occlusion plethysmography showing good correlation (Edwards *et al.* 1993). This was confirmed by DeBlasi *et al.* 1994) who also estimated forearm muscle oxygen consumption ($\dot{V}O_2$) non-invasively with NIRS. The measurements were made by inducing 50 mmHg venous occlusion and measuring the initial linear increase in deoxyhaemoglobin [d(Hb)/dt]. The values were similar to $\dot{V}O_2$ data obtained by other investigators using more established methods. Oxygen consumption has also been estimated from linear regression of the HbO_2 desaturation rate during ischaemia (DeBlasi *et al.* 1993, Hamaoka *et al.* 1996, Boushel *et al.* 1998).

Muscle blood flow measured by NIRS during exercise

We have recently used NIRS to measure muscle blood flow in the calf muscle during dynamic plantar flexion exercise and in the quadriceps muscles during knee extension and cycling (see also Boushel *et al.* 1997, 1999). During incremental exercise loads, ICG is injected into the venous circulation and blood withdrawn from an artery to record the arterial ICG curve. Changes in muscle tissue ICG concentration are determined by measuring light attenuation at several

wavelengths (775, 813, 850 and 913 nm), analysed with an algorithm incorporating the Modified Beer–Lambert Law and the wavelength specific extinction coefficient for ICG in mole cm^{-1}. As the measured light attenuation in tissue results not only from the ICG present during passage of the fraction of the injected bolus, but also from the oxy- and deoxy-haemoglobin present, the contribution of ICG to the light absorption signal is derived to quantify the absolute [ICG] in μmol. This is performed using a matrix operation (MATLAB) incorporating pathlength-specific extinction coefficients for each of the chromophores at each wavelength employed (Table 1).

When the amounts of tracer and the blood flow in the injection artery are known, the blood flow in the tissue region monitored by NIRS can be estimated from the peak of the recorded dye curve. Alternatively, blood flow can be calculated as the ratio of tissue ICG accumulation to the arterial input function which is the average [ICG] determined in the arterial blood over the same time period (Fig. 1). For any given time interval less than the time to reach peak tissue accumulation of tracer, the tissue receives the same fraction of the cardiac output as the fraction of the bolus received (Saperstein 1956). If it is assumed that the central dilution volume is constant (i.e. adequate mixing of ICG in the blood) and that the injection volume of ICG is accurately determined, then flow can be expressed by

$$\text{Flow(ml [100 ml]}^{-1}\text{ min}^{-1}) = \frac{k[\text{ICG}]_{\text{mt}}}{\int_0^t [\text{ICG}]_{\text{a}}\,\text{d}t}$$

where k is a constant reflecting the density of the tissue and the molecular weight of ICG for the conversion of ICG in moles to g L^{-1}; $[ICG]_m$ is the accumulation of ICG in muscle over time t expressed in μg; and $\int_0^t [ICG]_a\,dt$ is the time integral of the arterial [ICG] expressed as mg L^{-1}.

Assuming the tracer is evenly distributed within the monitored tissue volume when the curve reaches maximum height, the measured tracer concentration will reflect the blood flow in that region. Injection of the ICG bolus into the venous circulation provides sufficient admixture during passage through the heart and lungs before entry into the arterial and tissue microcirculation. To negate the potential influence of ICG recirculation on the calculation of flow, ICG accumulation is determined over less than half the mean transit time of the tracer, assuming that the first passage of the tracer occurs essentially within the time to $[ICG]_{max}$. Measurement of the initial rate of ICG accumulation in tissue eliminates the uncertainty of when the first and last part of the bolus passes the tissue. Three separate time intervals are used to calculate the blood flow for each ICG curve and the average value taken as representative of the entire curve.

This blood flow calculation requires three conditions: constant blood flow for the period of measurement, a linear dose–response relationship between the tracer concentration injected and that accumulated in tissue at each flow rate and that the tracer is not metabolized or retained in the tissue during the period of measurement (Lassen & Perl 1979). Accurate determination of arterial [ICG] by photodensitometry is performed by standard-curve blood ICG calibrations using known [ICG] in accurately measured volumes of each subjects' blood after each experiment.

Separate calibrations can be made by performing injections of known ICG volumes into a feed artery using a calibrated syringe. The recorded absorption curves are then converted to μg ICG by the matrix

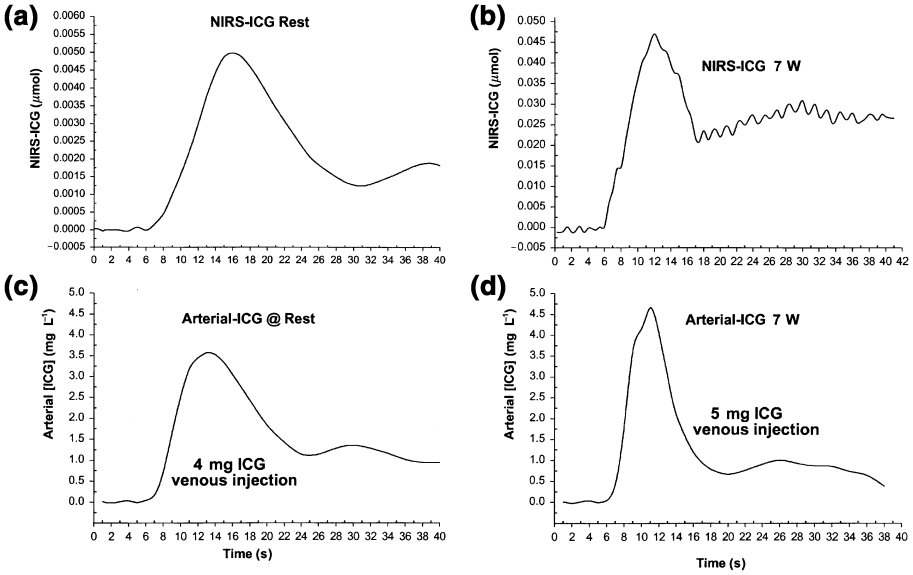

Figure 1 Representative tracings of indocyanine green dye (ICG) accumulation in calf muscle determined by near-infrared spectroscopy (NIRS-ICG) at rest (a) and during plantar flexion exercise at 7 W (b) in response to venous bolus infusion. (c, d) The corresponding arterial ICG curves determined by photodensitometry. Muscle blood flow is determined from the ratio of muscle ICG accumulation to the mean arterial [ICG] over the same time interval (see text).

operation. Then, coefficients are derived describing the ratio of peak tissue NIRS-ICG accumulation vs. ICG bolus volume for each subject at each exercise load. This calibration provides for a separate and independent analysis of the repeatability of NIRS-ICG responses at each exercise load and blood flow rate and for comparison between loads. Based on our experiments, a linear increase in tissue ICG coefficient occurs with progressive work rate and blood flow. This indicates that for a given arterial [ICG] infused, more ICG accumulates in muscle as blood flow increases and vice versa. The magnitude of blood flow is also significantly influenced by the rate of accumulation of the tracer in muscle relative to the arterial [ICG].

As a comparison with the blood flow values obtained by NIRS, leg blood flow has also been determined by the reverse-dye method using the same exercise protocol. As the blood flows derived by NIRS are expressed per unit tissue volume, MRI measurements of muscle volume can be made to express the reverse-dye blood flows in the same units (mL [100 mL^{-1}] min^{-1}). Blood flow during incremental plantar flexion exercise determined by both the NIRS and the reverse dye methods is presented in Fig. 2. A linear increase in blood flow is observed as a function of increasing work rate with both methods. However, with the reverse dye method, the flow rate at each work rate can vary significantly depending on the volume of muscle tissue presumed to be activated during exercise (Figs 2 and 3). An advantage of the NIRS blood flow method is that blood flow in a specific muscle region can be measured directly without estimates of active muscle volume. Furthermore, with the NIRS method the potential exists for mapping variations in blood flow within regions of a limb or muscle group.

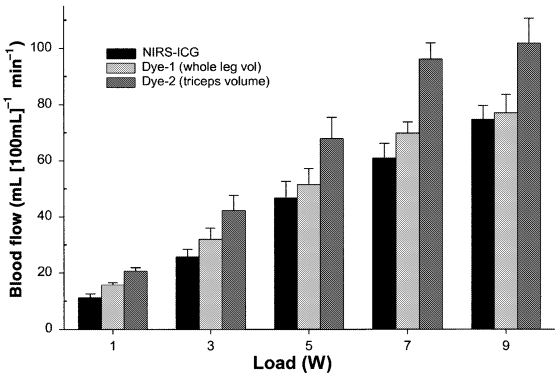

Figure 2 Blood flow response to incremental plantar flexion exercise determined by NIRS-ICG (dark-filled bars) and reverse dye combined with magnetic resonance imaging assessment of lower leg volume to express flow per 100 mL. Middle bars represent the reverse dye blood flow rate based on the muscle volume of the whole lower leg (volume = 1755 ± 91 mL, $n = 6$) and on the right, the blood flow rate assuming that only the triceps surae muscle group is activated during rhythmic plantar flexion (volume = 1330 ± 69 mL, $n = 6$).

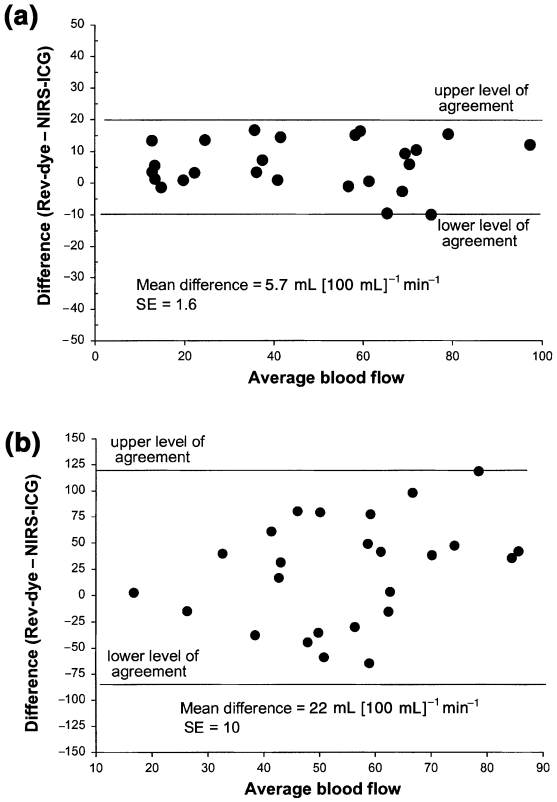

Figure 3 Altman plots showing the differences between the two blood flow methods and the upper and lower levels of agreement. As shown, the reverse dye method was on average 5.7 mL^{-1} (100 mL^{-1}) min^{-1} higher than the NIRS-ICG values when blood flow was expressed relative to the whole volume (a) and 22 mL higher based on only the triceps surae muscle volume measured by MRI (b).

NIR assessment of muscle oxygen metabolism in vivo

Near-infrared spectroscopy has been used to evaluate intracellular oxygenation and mitochondrial function at submaximal and maximal oxygen consumption *in vivo* (Duhaylongsod *et al.* 1993, DeBlasi *et al.* 1995, Nioka *et al.* 1998). Skeletal muscles deoxygenate to varying degrees during exercise in accordance with work intensity and level of training (Hansen *et al.* 1996, Nioka *et al.* 1998). Under some conditions, a close relationship between changes in the O_2 stores and CuA redox state can be demonstrated by NIRS. For instance, when the gracilis muscle of the dog is stimulated progressively until reaching $\dot{V}O_{2max}$, oxidized CuA decreases linearly as $\dot{V}O_2$ increases. At $\dot{V}O_{2\,max}$, the CuA oxidation state in this muscle approaches that found during ischaemia or at death (Fig. 4). As $\dot{V}O_2$ increases, progressive increases also occur in lactate efflux and lactate/pyruvate ratio from the muscle. Such results are consistent with

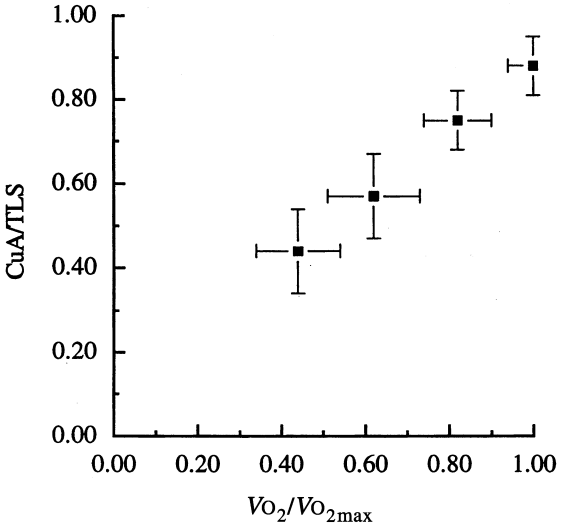

Figure 4 Relationship between mitochondrial oxidation state (CuA) and $\dot{V}O_2$ in the gracilis of the dog. Muscle stimulations at increasing frequencies were performed in conjunction with NIRS until steady-state $\dot{V}O_2$ was reached. Oxidation state of CuA was recorded and expressed as a fraction of the total reduction level (TLS) at death. $\dot{V}O_2$ expressed as a fraction of maximal oxygen uptake for each muscle ($\dot{V}O_{2max}$). Adapted from McCully *et al.* (1994).

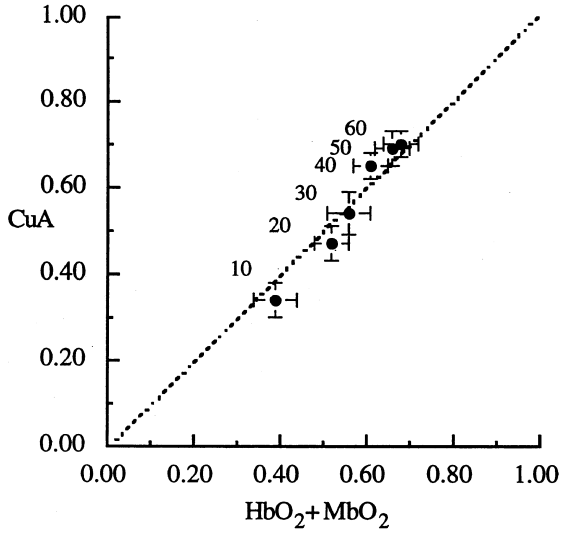

Figure 5 Relationship between mitochondrial oxidation state (CuA) and tissue O_2 stores (HbO_2 + MbO_2) in brachioradialis muscle of the human. Steady-state CuA values were obtained at progressively higher grip loads between 10 and 60% of the MVC (see small numbers on graph). Data for CuA and HbO_2 + MbO_2 expressed as fractions of maximal deoxygenation after 8 min forearm ischaemia.

the hypothesis that $\dot{V}O_{2max}$ in red skeletal muscles are limited by oxygen availability at the mitochondrial level.

In the human forearm, NIRS studies of the responses of the brachioradialis muscle have shown qualitatively similar relationships between O_2 store and CuA oxidation state (Fig. 5). Using graded handgrip exercise between 10 and 60% of maximal voluntary contraction (MVC), progressive deoxygenation of the muscle occurs accompanied closely by a decline in the oxidation state of CuA. The close agreement between the two signals, assuming no major optical artefacts are present, suggests that the metabolic needs of isometric contraction are met in accordance with a principle of discrete units of metabolism/O_2 store, analogous in concept to $\dot{V}O_2/Q$ units. It is important to recognize that the reflex-sympathetic tone capable of decreasing muscle oxygenation is not operating here. This response has been shown by NIRS to be abolished during handgrip exercise (Hansen *et al.* 1996). This quantum hypothesis and the size and composition of the apparent metabolic units will require further study in the future.

Muscle oxygenation under pathological conditions

In contrast to normal skeletal muscle, divergence between the O_2 stores and CuA oxidation state can be demonstrated under some pathological conditions, such as sepsis (Simonson *et al.* 1994). The basic principle can be illustrated by considering the effects of a metabolic inhibitor, such as cyanide, on muscle oxygenation. The infusion of cyanide into the muscle inhibits cytochrome oxidase by binding to the cytochrome haeme moiety of the enzyme. This event inhibits reduction of O_2 to water and results in an increase in the O_2 store (tHO_2 + MbO_2) but a decrease in the CuA oxidation state as electrons accumulate in the respiratory chain.

Similarly, any mitochondrial pathology that affects the ability of mitochondria to consume oxygen may result in desynchrony between CuA and the O_2 store (Simonson *et al.* 1994). In the dog gracilis muscle preparation, the relationship between CuA and the O_2 stores changes during muscle stimulation after treating the animal with endotoxin (LPS) (Fig. 6). At the same load, muscle deoxygenation increases less after LPS, but the inhibition of deoxygenation is greater for $tHbO_2$ + MbO_2 than for CuA. These results can be explained in at least two ways. If most of the decrease in O_2 store is owing to $tHbO_2$, then the difference induced by LPS suggests that it has resulted in a greater 'nutrient' concentration of HbO_2 in the muscle. On the other hand, if most of the change in O_2 store is owing to MbO_2, then the LPS effect suggests that the tissue PO_2 has been raised by LPS resulting in smaller changes in myoglobin saturation and redox state during stimulation. Of course, these two possibilities are not mutually exclusive. Both explanations may be true. However, neither of these explanations is the entire story, particularly with respect to the CuA oxidation state (Fig. 7). As Fig. 10 shows, the CuA response

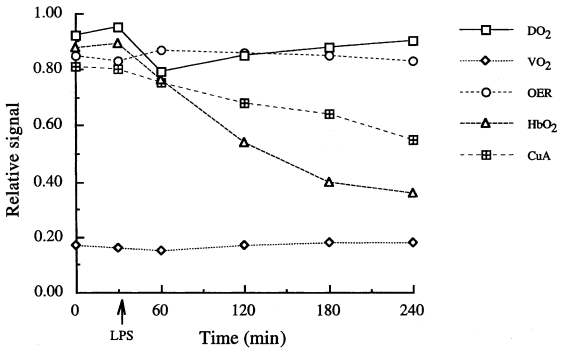

Figure 6 NIRS responses of dog gracilis muscle to repetitive muscle stimulation after LPS. Data are average values from six experiments. Standard errors were 10–15% for each parameter (not shown). Data are normalized to maximum signals except for $\dot{V}O_2$ which is expressed in ml O_2 min^{-1} g^{-1}. For NIRS signals (HbO_2 + MbO_2 and CuA) data were expressed relative to maximum deoxygenation or reduction at death. Note that LPS inhibits muscle deoxygenation and blunts the CuA reduction response to work despite constant oxygen delivery ($\dot{D}O_2$), oxygen extraction ratio (OER) and oxygen consumption ($\dot{V}O_2$).

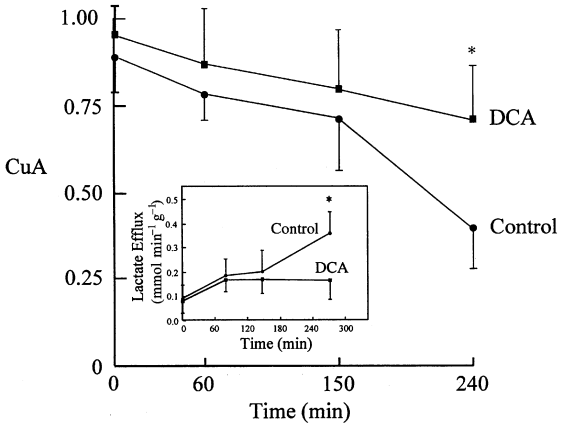

Figure 7 Effects of dichloroacetate (DCA) on mitochondrial oxidation state after LPS. The gracilis muscle of the dog was stimulated to near $\dot{V}O_{2max}$ beginning 30 min after intravenous infusion of *E. coli* LPS into the dog. CuA expressed as a fraction of TLC at death. The reductive response of CuA during stimulation is restored by DCA. Post-stimulation lactate efflux (inset) is also decreased after DCA.

during contraction can be partially restored by treatment of the muscle with dichloroacetate (DCA). DCA stimulates the pyruvate dehydrogenase complex in the mitochondria which has been inhibited by the effects of LPS. The presence of DCA allows electron flux in the respiratory chain to increase, thereby decreasing lactate accumulation and returning CuA to a less oxidized condition during the muscle contraction.

Other applications of NIRS to study pathological conditions in muscle also have been reported. For example, NIRS studies of peripheral vascular disease were explored as early as 1991 (Cheatle *et al.* 1991). Komiyama *et al.* (1994) attempted to identify different patterns of haemoglobin deoxygenation during exercise in patients with peripheral vascular disease and claudication. In another study, McCully *et al.* (1994) used NIRS to determine a time constant required to restore a normal muscle haemoglobin saturation profile after exercise in normal subjects and those with peripheral vascular disease. The rate of appearance of haemoglobin resaturation after exercise correlated with ankle-bronchial perfusion indices. These observations suggest that NIRS may have a diagnostic role in assessing the presence and extent of peripheral vascular disease in humans.

In summary, recent progress in near-infrared technology has enhanced our understanding of light propagation in tissues allowing for accurate assessment of changes in regional tissue oxygenation and blood flow. These parameters may provide valuable insights into basic mechanisms regulating microcirculatory O_2 transport and tissue O_2 utilization both at rest and during exercise in health and disease.

REFERENCES

Benaron, D.A. & Stevenson, D.K. 1994. Resolution of near infrared time-of-flight brain oxygenation imaging. *Adv Exp Med Biol* **345,** 609–617.

Boushel, R. & Ide, K., Pott, F. &. Secher, N.H. 1997. Muscle microvascular blood flow during exercise determined by near infrared spectroscopy. In: Photon Migration Tissues, *J Biomed Optics; SPIE Proc* **1,** 145–149.

Boushel, R., Langberg, H., Nowak, M., Olesen, J., Bülow, J. & Kjær, M. 1999. Blood flow in muscle and peritendinous tissue during exercise measured by near infrared spectroscopy and indocyanine green. *J Physiol* (submitted).

Boushel, R., Pott, F., Madsen, P. *et al.* 1998. Muscle metabolism from near infrared spectroscopy during rhythmic handgrip in humans. *Eur J Appl Physiol* **79** (1), 41–49.

Bucher, H.-U., Edwards, A.D., Lipp, A.E. & Duc, G. 1992. Comparison between near infrared spectroscopy and ^{133}xenon clearance for estimation of cerebral blood flow in critically ill preterm infants. *Pediatr Res* **33,** 56–60.

Cheatle, T.R., Potter, L.A., Cope, M. *et al.* 1991. Near-infrared spectroscopy in peripheral vascular disease. *Br J Surg* **78,** 405–408.

Colacino, J.M., Grubb, B. & Jobsis, F.F. 1981. Infra-red technique for cerebral blood flow: Comparison with ^{133}xenon clearance. *Neurol Res* **3,** 17–31.

De Blasi, R., Cope, M., Elwell, C., Safoue, F. & Ferrari, M. 1993. Noninvasive measurement of forearm oxygen consumption by near infrared spectroscopy. *Eur J Appl Physiol* **67,** 20–25.

DeBlasi, R.A., Fantini, S., Franceschini, M.A., Ferrari, M. & Gratton, E. 1995. Cerebral and muscle oxygen saturation measurement by frequency-domain near-infrared spectrometer. *Med Biol Eng Comput* **33,** 228–230.

DeBlasi, R.A., Ferrari, M., Natali, A., Conti, G., Mega, A. & Gasparetto, A. 1994. Noninvasive measurement of forearm blood flow and oxygen consumption by near-infrared spectroscopy. *J Appl Physiol* **76,** 1388–1393.

Duhaylongsod, F.G., Griebel, J.A., Bacon, D.S., Wolfe, W.G. & Piantadosi, C.A. 1993. Effects of muscle contraction on cytochrome a,a_3 redox state. *J Appl Physiol* **75,** 790–797.

Edwards, A.D., Richardson, C., van der Zee, P. *et al.* 1993. Measurement of hemoglobin flow and blood flow by near-infrared spectroscopy. *J Appl Physiol* **75,** 1884–1889.

Edwards, A.D., Wyatt, J.S., Richardson, C., Delpy, D.T., Cope, M. & Reynolds, E.O.R. 1988. Cotside measurement of cerebral blood flow in newborn infants by near infrared spectroscopy. *Lancet* **2,** 770–771.

Hamaoka, T., Iwane, H., Shimomitsu, T. *et al.* 1996. Noninvasive measures of oxidative metabolism on working muscles by near infrared spectroscopy. *J Appl Physiol* **81** (3)**,** 1410–1417.

Hampson, N.B. & Piantadosi, C.A. 1988. Near infrared monitoring of human skeletal muscle oxygenation during forearm ischemia. *J Appl Physiol* **64** (6)**,** 2449–2457.

Hansen, J., Thomas, G.D., Harris, S.A., Parsons, W.J. & Victor, R.G. 1996. Differential sympathetic neural control of oxygenation in resting and exercising human skeletal muscle. *J Clin Invest* **98** (2)**,** 584–596.

Hirako, M., Firbank, M., Essenpreis, M. *et al.* 1993. A Monte Carlo investigation of optical path length in inhomogenous tissue and its application to near-infrared spectroscopy. *Phys Med Biol* **38,** 1859–1876.

Jobsis, F.F. 1977. Noninvasive, infrared monitoring of cerebral and myocardial oxygen sufficiency and circulatory parameters. *Science* **198,** 1264–1267.

Komiyama, T., Shigematsu, H., Yasuhara, H. & Muto, T. 1994. An objective assessment of intermittent claudication by near-infrared spectroscopy. *Eur J Vasc Surg* **8,** 294–296.

Kuebler, W.M., Sckell, A., Habler, O. *et al.* 1998. Noninvasive measurement of regional cerebral blood flow by near-infrared spectroscopy and indocyanine green. *J Cereb Blood Flow Metab* **18** (4)**,** 445–456.

Kurth, C.D., Steven, J.M., Benaron, D. & Chance, B. 1993. Near-infrared monitoring of the cerebral circulation. *J Clin Monit* **9,** 163–170.

Lassen, N. & Perl, W. 1979. *Tracer Kinetic Methods in Medical Physiology*, pp. 76–101. Raven Press, New York.

McCully, K.K., Halber, C. & Posner, J.D. 1994. exercise-induced changes in oxygen saturation in the calf muscles of elderly subjects with peripheral vascular disease. *J Gerontol* **49,** B128–B134.

Nioka, S., Moser, D., Lech, G. *et al.* 1998. Muscle deoxygenation in aerobic and anaerobic exercise. In: Hudetz, A.G. & Bruley, D.F. (eds) *Oxygen Transport to Tissue XX*, ch. 8, pp. 63–70. Plenum Press, NY.

Piantadosi, C.A. 1993. Absorption spectroscopy for assessment of mitochondrial function *in vivo*. *Meth Toxicol* **2,** 107–126.

Piantadosi, C.A., Hall, M. & Comfort, B.J. 1997. Algorithms for *in vivo* near-infrared spectroscopy. *Anal Biochem* **253,** 277–279.

Piantadosi, C.A., Hemstreet, T.M. & Jobsis-Vander Vliet, F.F. 1986. Near-infrared spectrophotometric monitoring of oxygen distribution to intact brain and skeletal muscle tissues. *Crit Care Med* **14,** 698–706.

Roberts, I., Fallon, P., Kirkham, F.J. *et al.* 1993. Estimation of cerebral blood flow with near infrared spectroscopy and indocyanine green. *Lancet* **342,** 1425.

Saperstein, L.A. 1956. Fractionation of the cardiac output of rats with isotopic potassium. *Circ Res* **4,** 689–692.

Simonson, S.G., Welty-Wolf, K., Huang, Y.-C.T. *et al.* 1994. Altered mitochondrial redox responses in gram negative septic shock in primates. *Circ Shock* **43,** 34–43.

Skov, L., Pryds, O. & Greisen, G. 1991. Estimating cerebral blood flow in newborn infants: comparison of near infrared spectroscopy and ^{133}xe clearance. *Pediatr Res* **30,** 570–573.

Wray, S., Cope, M., Delpy, D.T., Wyatt, J.S. & Reynolds, E.O. 1988. Charaterization of the near infrared absorption spectra of cytochrome aa_3 and haemoglobin for the non-invasive monitoring of cerebral oxygenation. *Biochim Biophys & Acta* **933** (1)**,** 184–192.

Wyatt, J.S., Cope, M., Delpy, D.T. *et al.* 1990. Measurement of optical path length for cerebral near-infrared spectroscopy in newborn infants. *Dev Neurosci* **12,** 140–144.

van der Zee, P., Cope, M., Arridge, S.R. *et al.* 1992. Experimentally measured optical path lengths for the adult head, calf and forearm and the head of the newborn infant as a function of interoptode spacing. *Adv Exp Med Biol* **316,** 143–153.

